NATIONAL AERONAUTICS AND SPACE ADMINISTRATION

Research Grant NGR-09-005-025

Diagnostics of Accelerating Plasma

3rd Semi-Annual Progress Report

March 1, 1967 - August 31, 1967

Report No. 67-029

by

T. N. Lie, A. W. Ali,

and

C. C. Chang

August 31 , 1967

Department of Space Science and Applied Physics
The Catholic University of America
Washington, D. C. 20017

Forward

Th present semi-annual progress report, consisting of the contents of this volume and a separate report entitled "Structure of Magnetohydrodynamic Shock Wave", covers the period 1 March 1967 through 31 August 1967. The separate report "Structure of Magnetohydrodynamic Shock Wave" is essentially a Ph.D. thesis by C. K. Liu of this laboratory and is concerned with the studies of the plane magnetohydrodynamic shock wave of a rarefield, fully-ionized plasma. Portion of the work included in the present report were presented at the AIAA Conference on Electric Propulsion and Plasmadynamics at Colorado Springs, Colo. (11 - 13 September, 1967) and the APS Topical Conference on Pulsed High Density Plasma at Los Alamos, N.M. (19 - 22 September 1967).

We wish to acknowledge the assistance given by M. J. Rhee and J. Williams, graduate assistants and also the advice given by Mr. E. A. McLean of the Naval Research Laboratory, Washington, D.C.

ABSTRACT

The electric polarity effect observed in the coaxial plasma accelerator has no convincing explanation so far. This report deals with a possible mechanism for the unexpected behavior of the current-sheet with some experimental evidences. A considerable level of pre-ionization, a discharge current ahead of the current-sheet, and an axial current along the anode surface were observed in both parallel plate and coaxial plasma accelerators. The polarity effect in the coaxial accelerator is not likely due to a hydromagnetic origin but is inferred to be primarily a discharge phenomena caused by unusually high anode sheath voltage and lower cathode fall within a current-sheet. The current-sheet produced with the hydrogen filling behaves differently from non-hydrogen gas filling as was shown in a previous report and this is explained with the proposed mechanism. The calculation of partition functions of He II and C II was carried out as a preliminary study of radiation loss and the result is shown.

TABLE OF CONTENTS

LIST OF ILLUSTRATIONS

I. Introduction

In the previous semi-annual report, some of the electric polarity effects observed in coaxial accelerators are shown. The existence of the polarity effect in this type of plasma accelerator is very important because it contradicts the existing theoretical model. There exists some confusion and disagreement about the current-sheet obtained by previous investigators[1] [2] [3] [4]. The main cause of this disagreement appears to be due to the fact that the accelerators used by previous workers are not operated under identical conditions. The conditions such as accelerator geometry, species of working gas, electric polarity, the way of introducing a gas into the system are known to affect the behavior of the current-sheet. An analytical model of the current-sheet acceleration, which covers the effects of these conditions is not available and obviously some physical processes going on within a coaxial plasma accelerator remain undiscovered.

The present investigation is an experimental study to improve understanding of the current-sheet behavior and to sort out the effects caused by various conditions of operation. The electric polarity effect in the coaxial accelerator represents essentially the same tendency as the current-sheet tilt in the parallel plate plasma accelerator. The pre-ionization phenomena observed in the plasma accelerators of coaxial as well as parallel plate geometry are shown in an attempt to give an explanation to the polarity and pressure dependent features of the current-sheets,

The partition functions of He II and C II are calculated as these are needed for the estimation of the radiation loss. The result is shown in section V.

II. Pre-ionization in Coaxial and Parallel Plate Plasma Accelerators.

A. Pre-ionization in Parallel Plate Accelerator

The parallel plate plasma accelerator used in this investigation consisted of a pair of copper plates 6 cm wide, 8 cm long and 3.5 cm apart enclosed in a quartz tube 6 inches in diameter. (See Fig. 1) The discharge was driven by a $15 \mu F$ capacitor charged to 10 KV and triggered by a pressurized switch. The rise-time of the discharge current was about $1.8 \mu sec.$

The question of the existence of appreciable pre-ionization ahead of the propagating current-sheet in the pulsed plasma accelerator is important since the presence of the ionized gas may significantly alter the expected current-sheet behavior, The spectral radiation emitted from the pre-ionized gas was detected with monochrometers (Fig. 1) and the photoelectric signals were displayed on an oscilloscope simultaneously. Figure 2 illustrates the signal waveforms and the time correlation between them at various locations in the electrode gap when the accelerator is filled with helium gas at $p = 0.5$ Torr. $x = 3.3$ cm, $x = 1.75$ cm and $x = 0.2$ cm correspond to the locations which are near the anode, the mid-point of the gap and near the cathode, respectively, The dotted lines indicate the peak which corresponds to the current-sheet. Immediately evident are the signals of He I 5876 $\overset{o}{A}$, He I 4471 $\overset{o}{A}$, O II 3135 $\overset{o}{A}$ and N III 3367 $\overset{o}{A}$ lines which start at the very beginning of the discharge current and whose amplitudes are comparable to those at the curaent-sheet which arrives at a much later time. None of the He II lines were observed here but there is reason to believe that a considerable amount of pre-ionization of ambient gas atoms takes place. The signal wave-shapes near the anode region indicate that the current-sheet is not well defined and that the level of pre-ionization seems to be even higher whereas the current-sheet near the cathode region is very peaky and sharply defined. The pre-ionization is detected not only in the electrode gap but also as far as 20 cm beyond the electrode end. Nitrogen ($p = 0.07 - 0.2$ Torr) and argon ($p = 0.05 - 0.15$ Torr) were also used as work-

Insulator ———

Electrodes

8 cm ——

6 cm ——

Insulating
sheet

Quartz tube

To switch
and
Capacitor

Monochromator

x

+

z

y

−

Lens

Monochromator
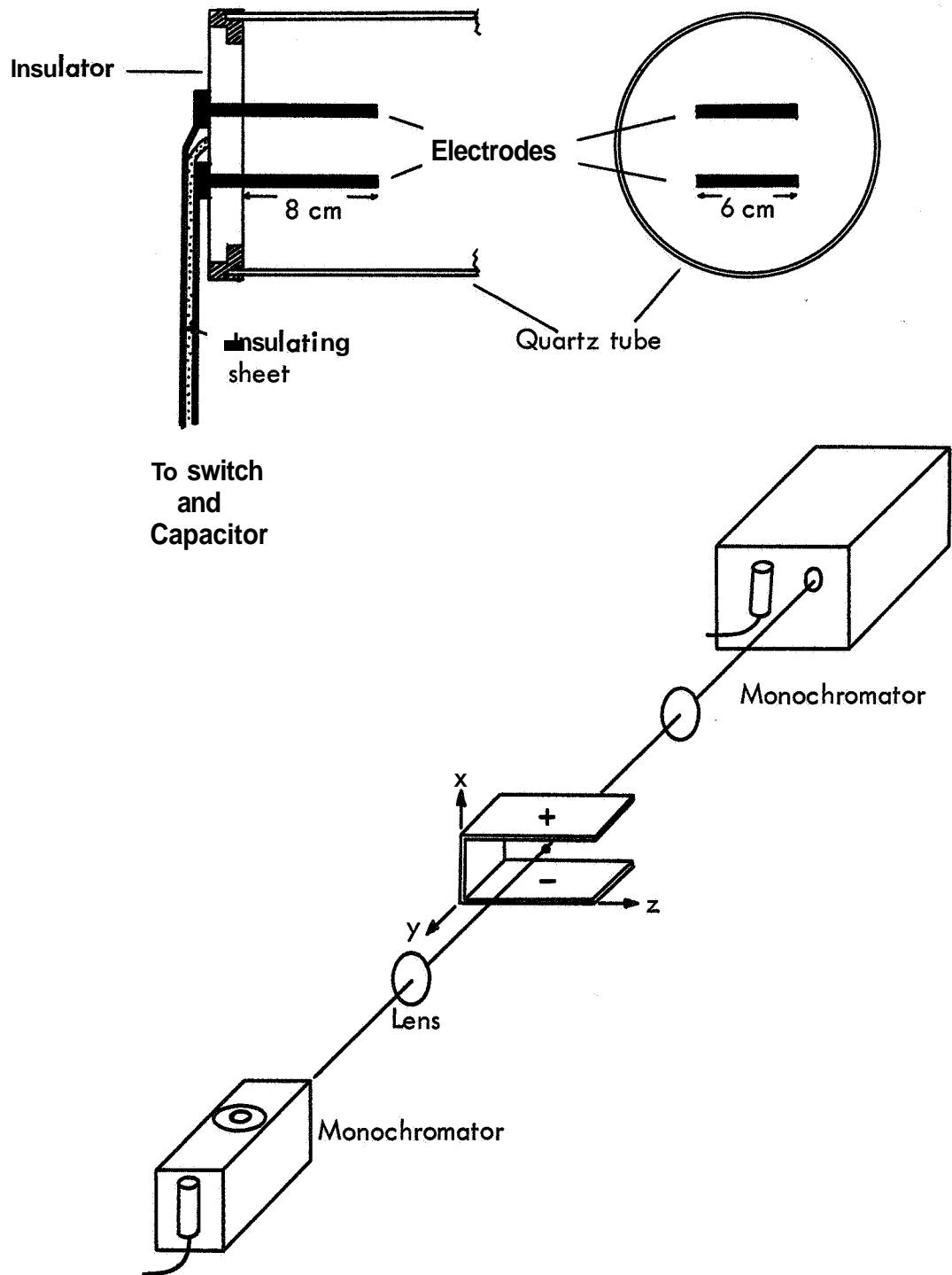
FIG. 1   SCHEMATIC DIAGRAM OF PARALLEL PLATE PLASMA
ACCELERATOR AND OPTICAL ARRANGEMENT
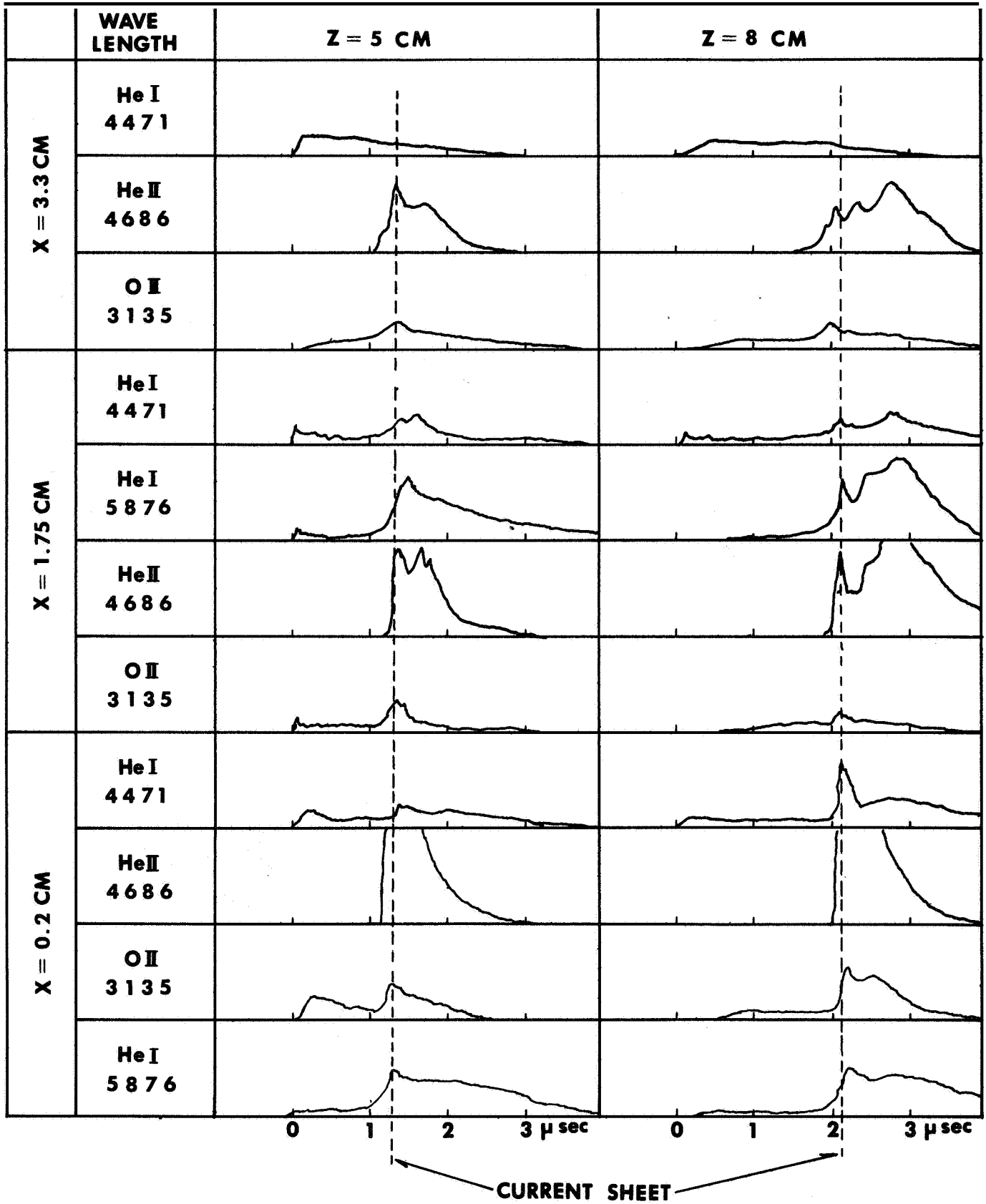
FIG. 2 WAVE-FORMS OF PHOTOELECTRIC SIGNALS AT VARIOUS LOCATIONS OF ELECTRODE GAP AND THEIR TIME CORRELATION (He at p = 0.5 Torr)

ing gases and the typical oscillograms obtained are shown in Fig. 3. As can be seen, essentially the same tendency occurs here as in the case of helium filling and the spectral lines from ionized species such as N II, N III and A II are detected in the pre-ionized media. In the case of hydrogen gas filling at pressures greater than 0.3 Torr, however, no pre-excited hydrogen lines were detected even with a wider slit width of the monochromator and the impurity lines which would be detected with the other working gases were not observed.

B. Coaxial Accelerator

The coaxial plasma accelerator consisted of two cylindrical electrodes, the inner electrode being 1.6 cm in diameter by 12 cm long and the outer electrode being 5 cm in diameter by 6.5 cm long. The electrodes were enclosed in a 4-inch diameter quartz tube for optical observation. The quarter cycle time of the discharge was about $0.6\ \mu$ sec. Two monochromators were so aligned in the plane perpendicular to the accelerator axis and 1 mm from the outer electrode end that they each pick up the radiations from different radial locations of the accelerator. A schematic diagram of the accelerator and the optical arrangement is shown in Fig. 4.

A considerable level of pre-excitation and pre-ionization in the cold gas ahead of the current-sheet has also been detected in the coaxial accelerator. Typical examples of such photoelectric signals and their time correlation in the case of helium filling are shown in Fig. 5. The pre-ionization signals are particularly high in the vicinity of the outer electrode when the polarity of the center electrode is negative. When the polarity is reversed, the pre-arriving signal at the outer electrode (negative) is usually a very sharp pulse at the beginning of the discharge and decays rapidly. Argon and nitrogen also show essentially the same signal (a typical example is shown in Fig. 6).
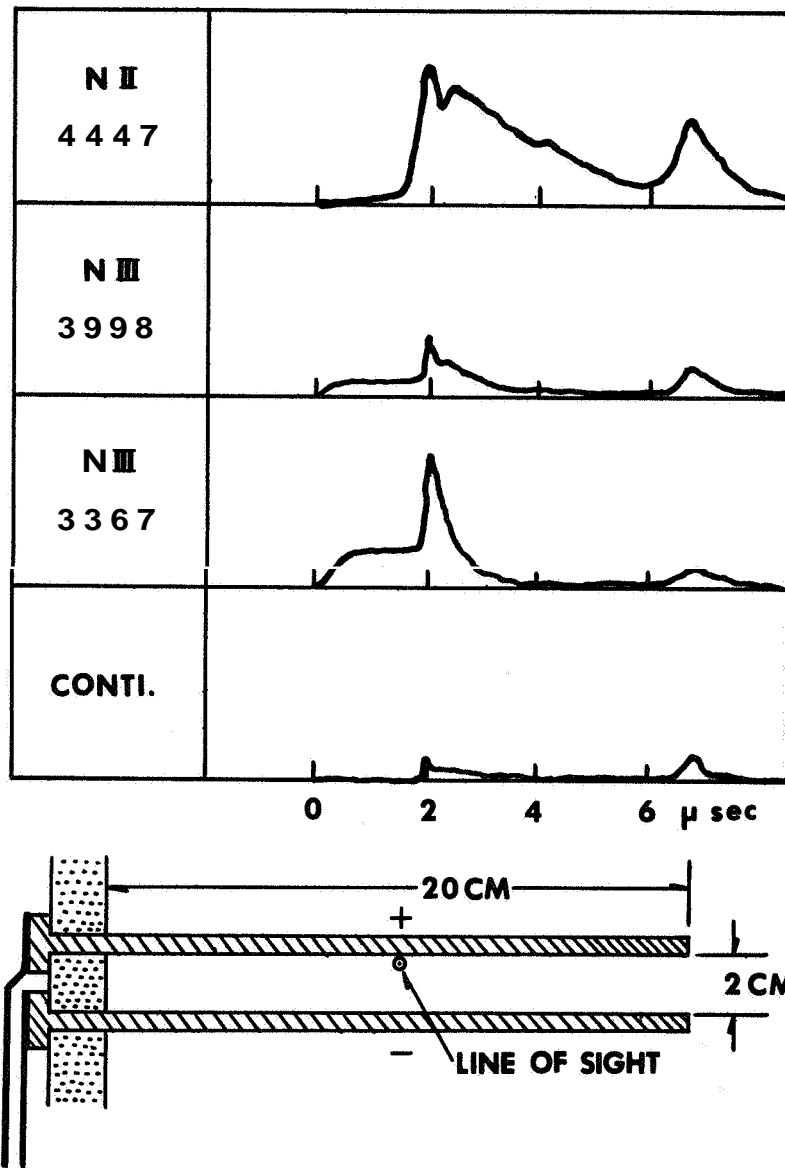
FIG. 3 ACCELERATOR GEOMETRY AND PRECURSOR SIGNALS OF IONIC LINES OF NITROGEN (N$_2$ at p $=$ 0.07 Torr)

MONOCHROMATOR

COAXIAL PLASMA
ACCELERATOR

MONOCHROMATOR

r_1

r_2

10 μf

9 KV

0.6 μsec RISE TIME

1 mm

LINE OF SIGHT

5 cm

1.6 cm

4.5 cm
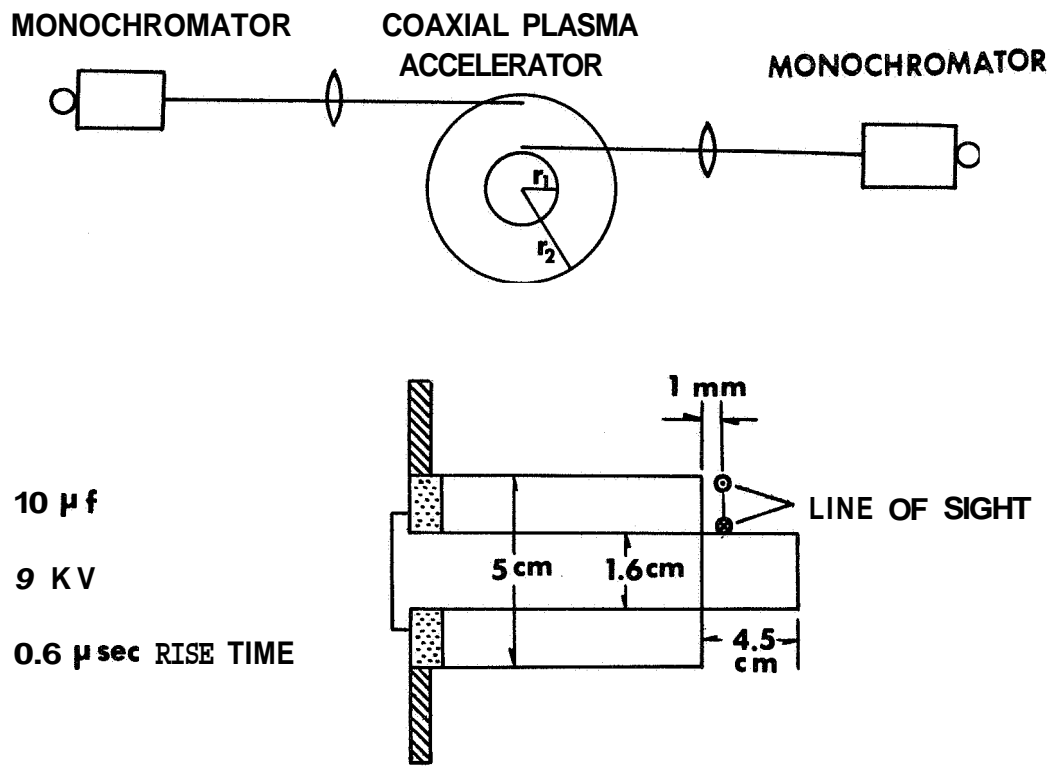
FIG. 4 GEOMETRY OF COAXIAL PLASMA ACCELERATOR AND OPTICAL ARRANGEMENT

CENTER ELECTRODE

NEGATIVE   POSITIVE

HeII 4686

HeII 4686 $r = r_1$

HeI 4471 r_2

C III 2297 r_2

N III 3367 r_2

                   e

0   1   2   3 µsec

0   1   2   3 µs
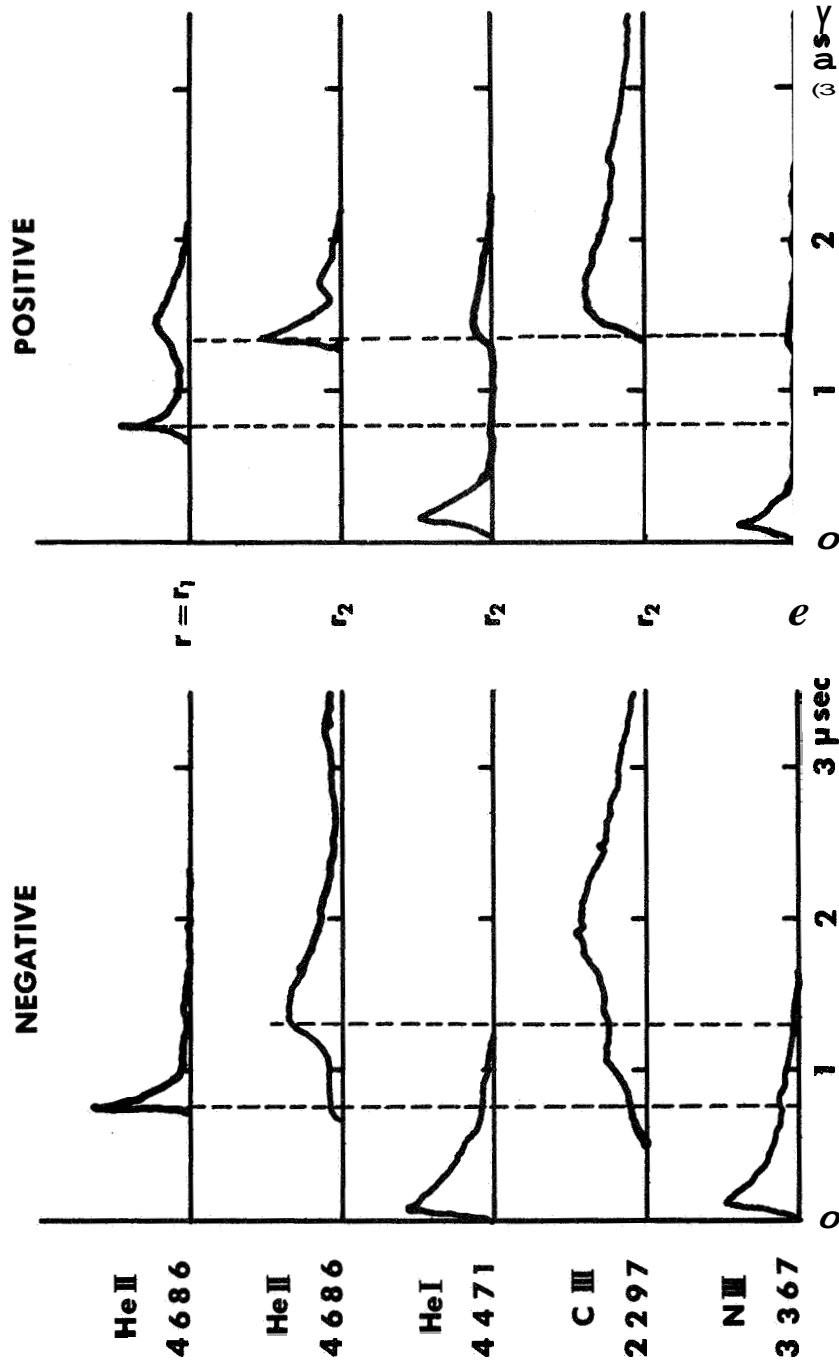
He : P = 0.5 TORR

FIG. 5   PHOTOELECTRIC SIGNALS AND THEIR TIME CORRELATION SHOWING PRECURSOR SIGNAL
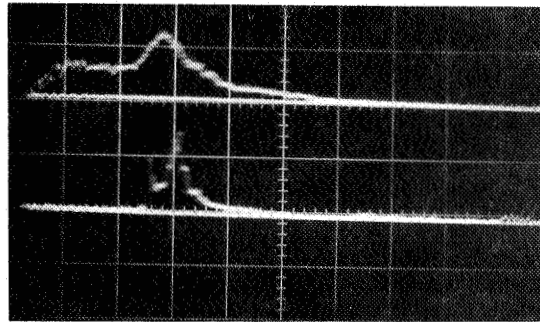
A II   4 8 0 6 Å
P = 0.05 Torr
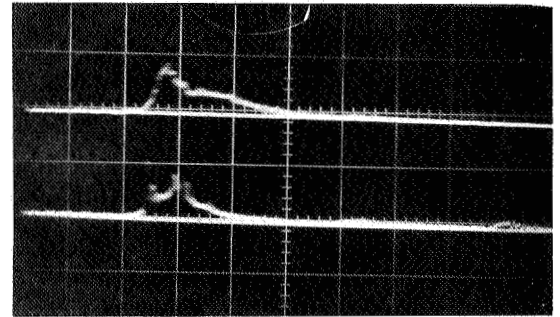
A III   3 3 3 6 Å
P = 0.05 Torr
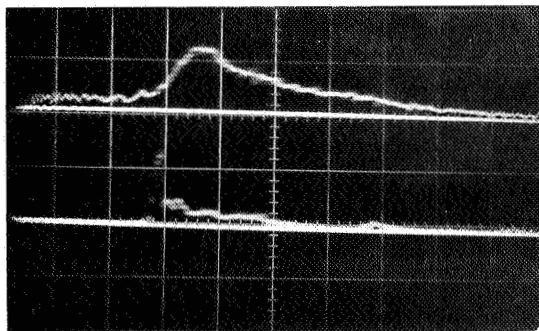
A II   4 8 0 6 Å
P = 0.15 Torr
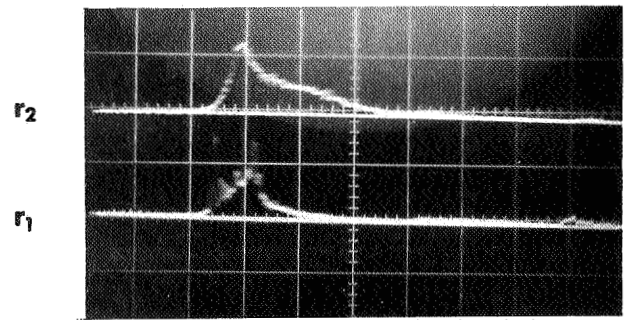
A IV   3 0 7 7 Å
P = 0.05 Torr

0.5 μ sec/div
Argon — Gas

FIG. 6   OSCILLOGRAMS OF PHOTOELECTRIC SIGNALS OF IONIC ARGON LINES
TAKEN SIMULTANEOUSLY AT $r = r_1$ and $r = r_2$ WITH THE CENTER
ELECTRODE NEGATIVE (ARGON AT $p = 0.05$ and 0.15 Torr)

A magnetic probe coil was found to have sufficient sensitivity to respond to the current carried by the pre-ionized gas in both the accelerators. Figure 7 shows the oscillograms obtained with helium and hydrogen filling in the coaxial accelerator. The current carried in the media ahead of the current-sheet is sensitively varied with the filling pressure of a gas and one notices that the radial current ahead of the current-sheet is small in the case of hydrogen filling. In the parallel plate accelerator, gas pressure dependence of the pre-current is not as sensitive as in the case of coaxial accelerator; however, it again shows a definite difference between the hydrogen and the non-hydrogen gas filling. The magnetic probe signals obtained are in good agreement with the photoelectric signals of the spectral lines and indicate the existence of considerable discharge current ahead of the main current-sheet particularly when the filling pressures are low.

D. Mechanism

Obviously, the pre-ionization is not related to the initial heavy current discharge near the insulator and has nothing to do with the radiation emitted by the main discharge. This was confirmed with a simple experimental arrangement as shown in Figure 8, i.e., a circular insulating disk was inserted into the annulus of the coaxial accelerator. Photoelectric signals of the He I 4471 $\overset{o}{A}$ line observed near the outer electrode end with and without the disk show clearly copious precursor signals at the beginning of the main discharge.

The electron density of the pre-ionized gas has not been determined. A check of the line width of the He I 4471 $\overset{o}{A}$ line indicates $N_e < 10^{15} cm^{-3}$ and an educated guess of the density from the total line intensity is $N_e \sim 10^{12} - 10^{14} cm^{-3}$. It is not clear whether the precursor observed in this experiment has a definite propagation velocity or not, however, it would be greater than $10^9 cm/sec$ if the velocity has a meaning., Recently Lubin[5] developed

He — GAS   P = 0.4 Torr   He — GAS   P = 1 Torr

H₂ — GAS   P = 0.5 Torr   H₂ — GAS   P = 1 Torr

0.5 μ sec/div
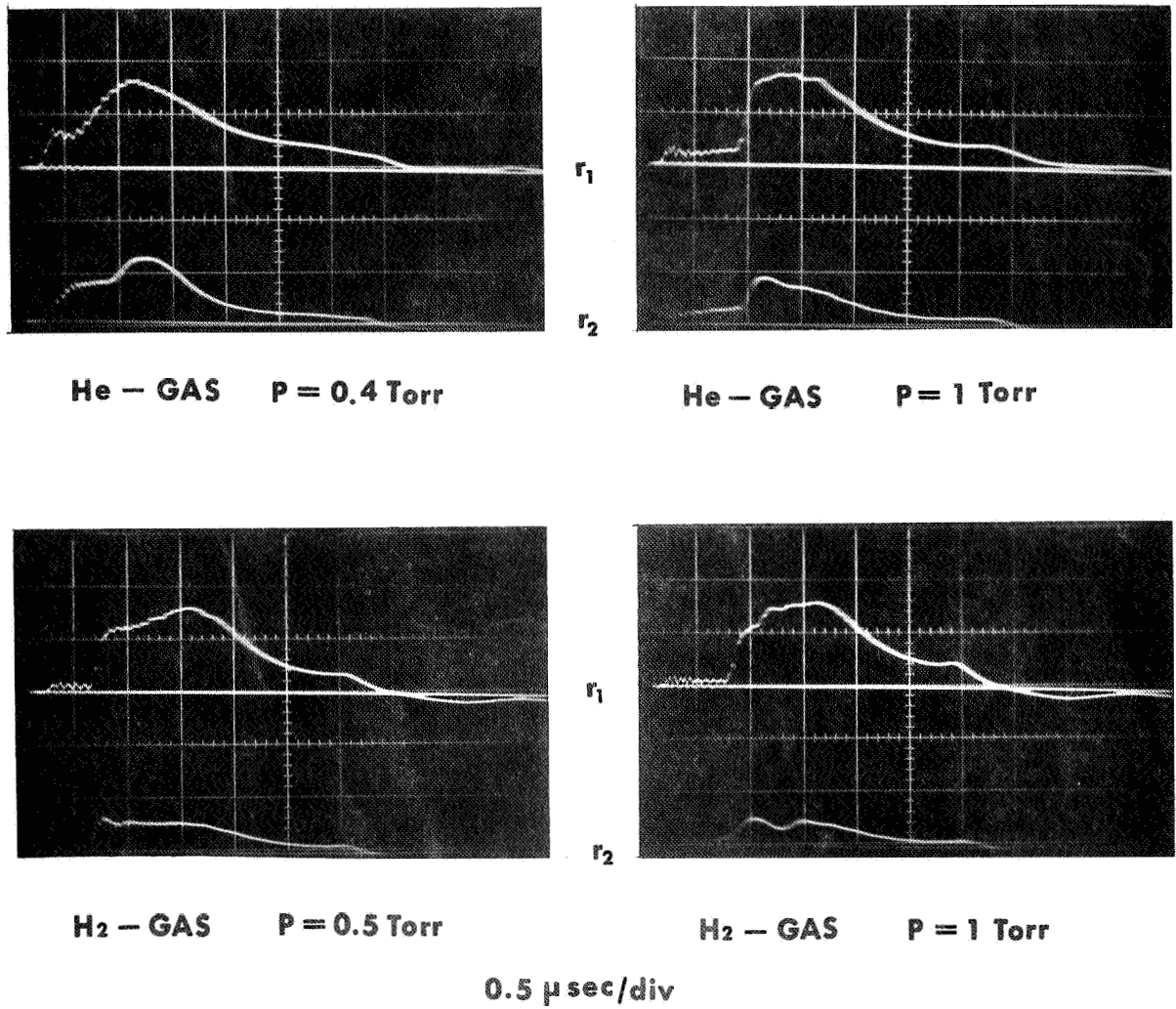
FIG. 7 OSCILLOGRAMS OF MAGNETIC PROBE SIGNALS TAKEN S MULTANEOUSLY
AT $r = r_1$ and $r = r_2$ WITH THE CENTER ELECTRODE NEGATIVE (Heat $p = 0.4$
and 1 Torr, H_2 at $p = 0.5$ and 1 **Torr**)

CIRCULAR
PLASTIC DISK

LINE OF SIGHT

He I

4471

WITHOUT DISK

CURRENT SHEET

WITH DISK

0   1   2   3   4   5 µ sec
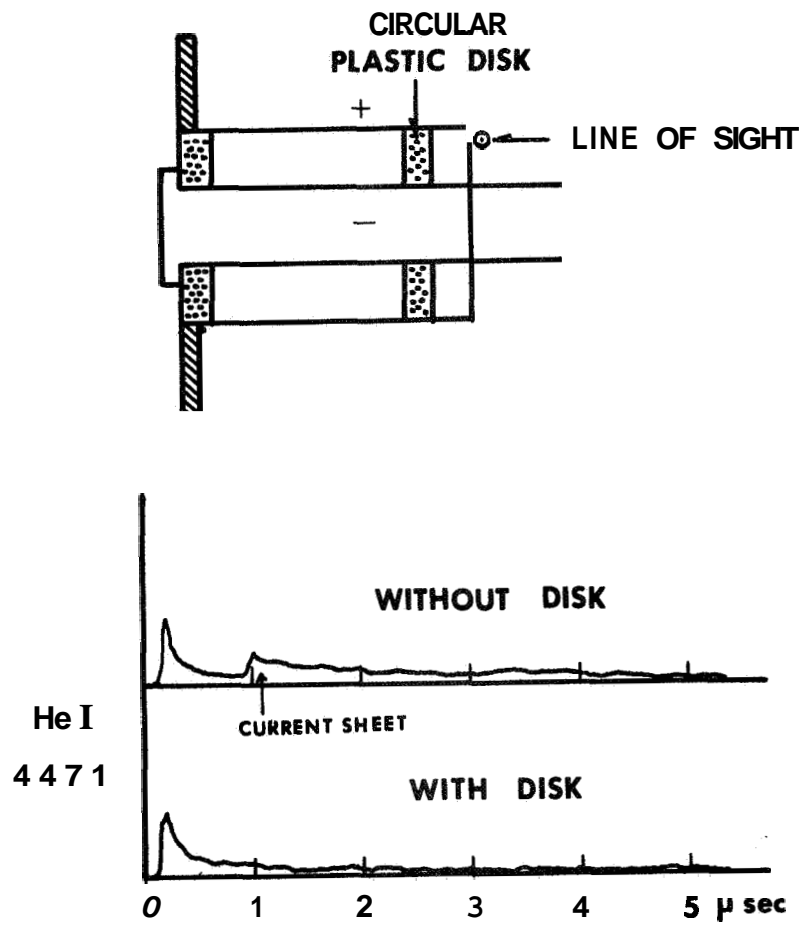
FIG. 8   PRECURSOR SIGNAL WITH AND WITHOUT AN INSULATING DISK IN
ANNULUS OF COAXIAL ACCELERATOR (He at p = 0.5 Torr)

a precursor theory which seems to be in good agreement with his measurements on an electro-magnetic shock tube of T-configuration.   According to the result, the precursor has a wave-like structure and an electron density of $10^{11} cm^{-3}$.   It is not clear whether the pre-ionization phen-omena observed in the present investigation is the same kind as observed in the T-tube.   Whatever its propagation mechanism may be,   the cause of the ionization ahead of the current-sheet is due to a discharge between the electrodes which is extended out in the forward direction.   When the accelerator is triggered no doubt the whole length of the electrode gap undergoes Towsend pre-breakdown discharge, which carries very little current and as the ionization grows rapidly, with certain secondary processes, the whole electrode gap turns to breakdown. As $\dfrac{dI}{dt}$ increases the massive current tends to flow through the least inductive path-near the insulator $-$ but there also exists a discharge current ahead of the current-sheet, which is an appreciable fraction of the current at the sheet, as was shown in the probe data,

III. Current-Sheet at Electrodes

A.   Cathode region

One of the polarity dependent features observed in the coaxial accelerator is that the bright layer of luminosity covering the center electrode surface extends all the way to the insulator when the center electrode has a negative polarity,   This has also been observed as a dense plasma layer on the negative electrode surface in the parallel plate accelerator[6] [7] and it was inferred that at least a fraction of the discharge current may be carried by this layer instead of being carried by the electrode itself.   Evidence which supports this assumption is shown in Fig. 9.   Figure 9a is a framing photograph which shows the moment when the luminosity front is about 2 cm beyond the center electrode tip.   In the case of a positive center electrode, the cursent-sheet pinches toward the axis immediately beyond the inner electrode forming an

ACCELERATOR #1 B

(a)

ACCELERATOR #1 C

(b)

(c)
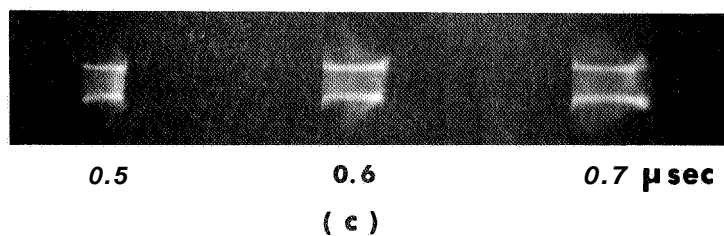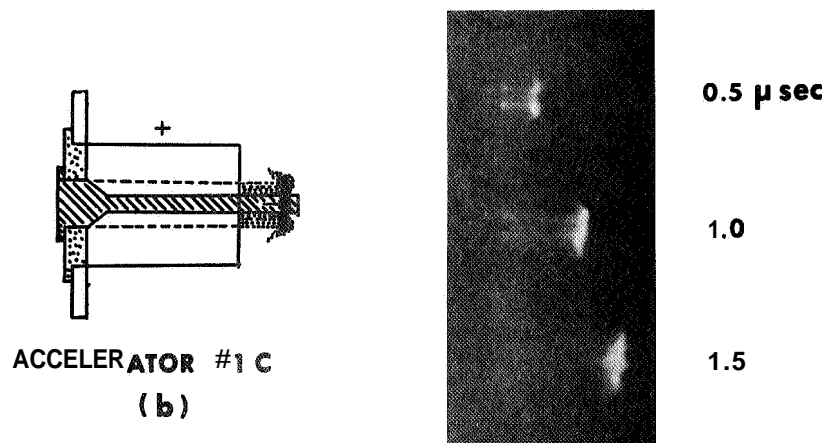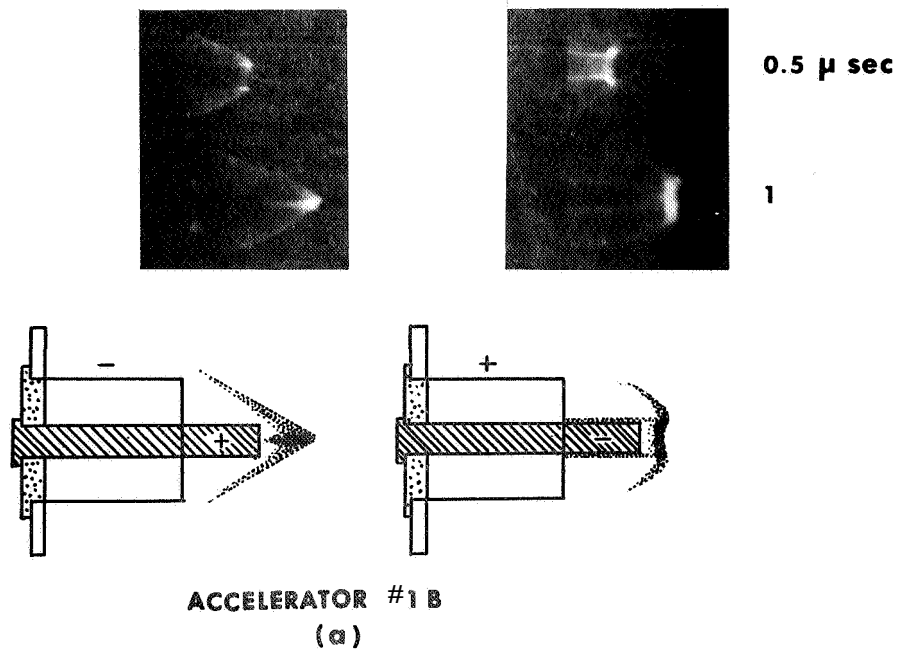
FIG. 9 (a) FRAME PHOTOGRAPHS OF LUMINOUS FRONT AT ELECTRODE END SHOWING
CURRENT PATH FOR BOTH POLARITIES   (b) FRAME PHOTOGRAPH SHOWING
A THICK PLASMA LAYER ON THE CATHODE SURFACE (ACCELERATOR # 1C)
(c) DENSE PLASMA LAYER ON THE CATHODE SURFACE (ACCELERATOR #1B)

-14-

arrowhead-like configuration. When the center electrode is negative, however, the current-sheet does not collapse to form a pinched plasma stem but the thin luminous layer on the cathode extends its path just beyond the center electrode end. This state lasts until the front tip of the plasma is 1 to 2 cm from the electrode end where the current-sheet is destroyed in an un-organized manner and finally pinches toward the axis, Figure 9b is a photograph taken with a coaxial accelerator where the center electrode was modified so as to have a larger cross-section at the insulator region than at the remaining part of the electrode., The photograph shows that the plasma layer on the center electrode is much thicker. The above observations, although only qualitative in nature, indicate that a considerable portion of the discharge current is carried by the plasma layer on the cathode. Phis means that the cathode surface acts as if it were a resistive conductor or nearly as an insulator to the cusrent-sheet.

B. Anode region

The propagating current-sheet in the vicinity of the anode wall is not well defined as was seen in both photoelectric and probe signals. Fig. 10 shows oscillograms of the miniature Wogowski coil signals obtained at $r = r_2$ (radius of the outer electrode) and $r = r_1$ (radius of center electrode) in the coaxial uccelerator. In the case of helium, argon and nitrogen filling, always $J > J_{r_1}$ ahead of the current-sheet indicating there is a current of axial component at the positive outer electrode. On the other hand, hydrogen showed a sharp rise at the current-sheet even at $r = r_2$" The existence of the surface current along the anode in both accelerators can be demonstrated with framing photographs and this is shown in Fig. 11. The aperture of the image converter camera was wide open to admit enough light for the photographs and part of the quartz tube was covered to shield it from the intense light of the current-sheet in the parallel plate accelerator. The first frame of the photograph is exposed when the current-sheet is still

J_{r_1} $\perp$ 38 Ka/Cm²

J_{r_2} $\perp$ 19 Ka/Cm²

He : P = 0.5 Torr

J_{r_1} $\perp$ 38 Ka/Cm²

J_{r_2} $\perp$ 19 Ka/Cm²
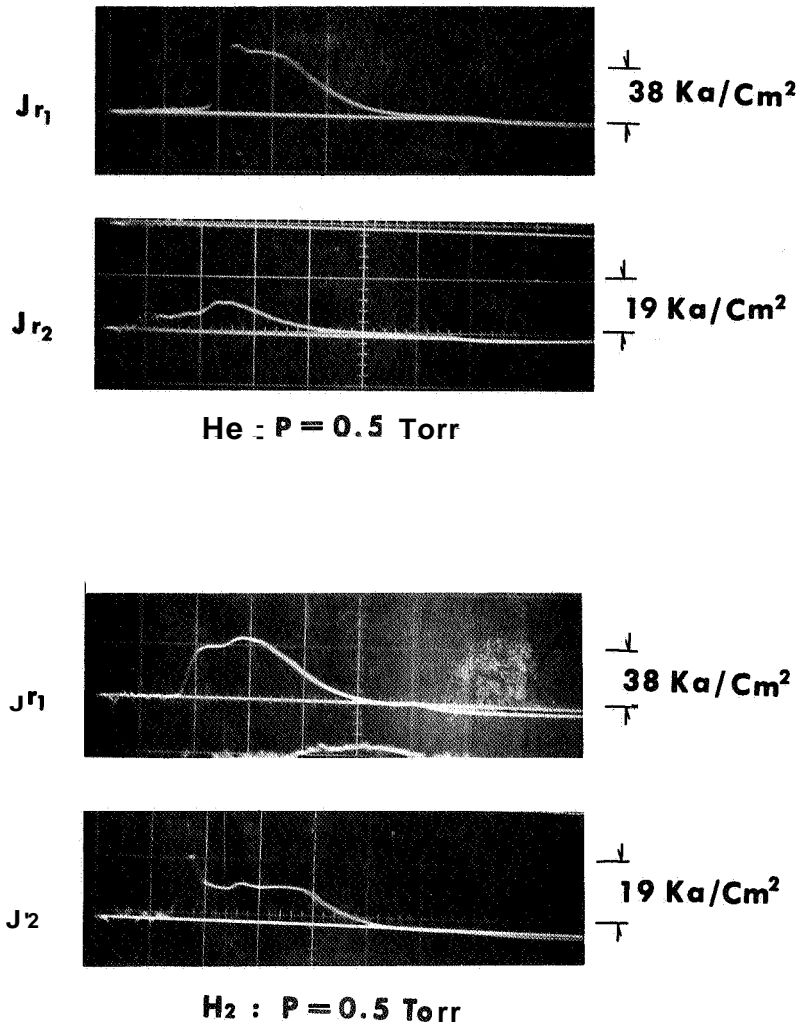
H₂ : P = 0.5 Torr

FIG. 10 OSCILLOGRAMS OF SIGNALS FROM MINIATURE PRGOWSKI'S COIL SHOWING CURRENT DENSITY AT $r = r_1$ and $r = r_2$ (He at $p = 0.5$ Torr AND H_2 at $p = 0.5$ Torr)

A : P = 0.1 TORR

PARALLEL
PLATE
SYSTEM

0.7   0.6   0.5

0.2   0.1   0 μ sec

COAXIAL
SYSTEM

0.2   0.1   0 μ sec

N₂ : P = 0.2 TORR

CENTER ELECTRODE POSITIVE
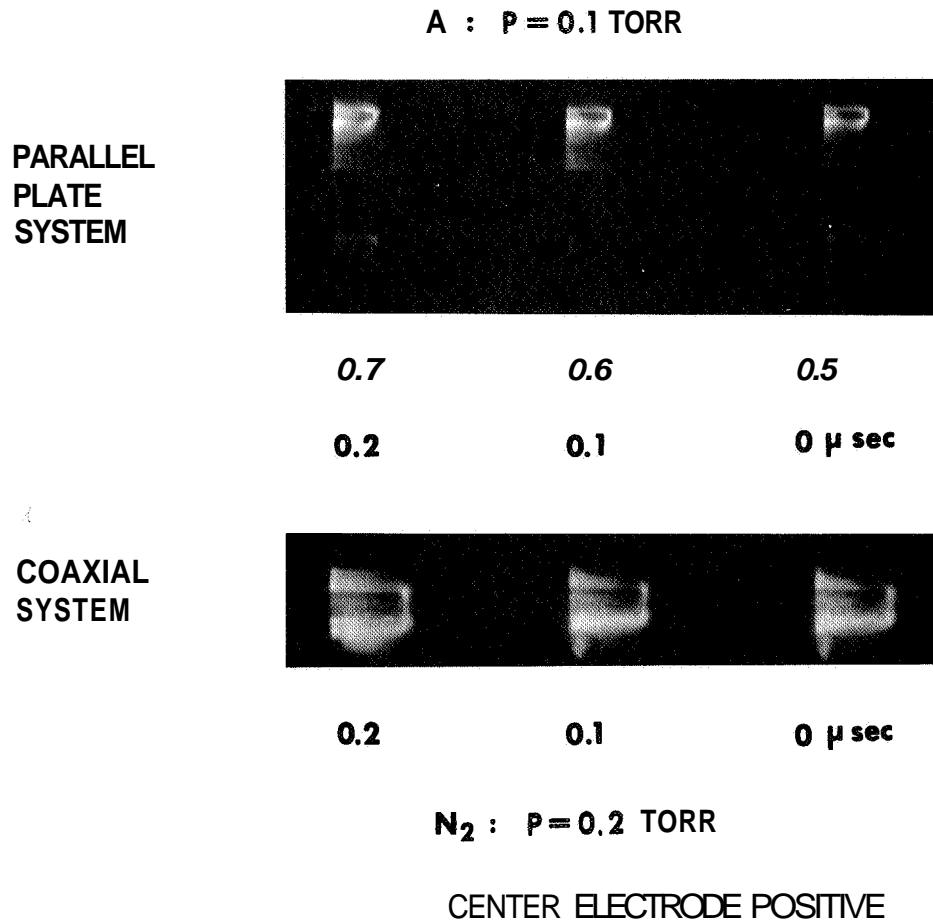
FIG. 11   FRAME PHOTOGRAPHS TAKEN PRIOR TO THE EMERGENCE OF CURRENT-SHEET
SHOWING LUMINOSITY COVERING ENTIRE LENGTH OF CATHODE IN EARLY
STAGE OF DISCHARGE

near the insulator. **As** can be seen, a luminosity covers the whole surface of the anode at this

moment and gets brighter until the current-sheet finally appears. This is true for the coaxial

accelerator as can be seen in the photograph (in this case, the center electrode was positive).

These framing photographs together with the Rogowski coil data imply that as soon as the current-

sheet is formed near the insulator, the current-sheet near the anode begin to have axial com-

ponents in the forward direction along the electrode.

C. Discharge current pattern near the Electrodes

Figure 12 shows a simplified pattern of current path of the current-sheet described

in previous sections. It appears to be unusual current path near the anode and cathode re-

spectively, This is likely due to the existence of an abnormally high anode sheath voltage

whereas the cathode fall is very small, These have been measured by Lovberg[8] for the

parallel plate accelerator previously. The current-sheet near the anode then seeks its current

path forward (and backward) through the already ionized media ahead, In the ordinary electronic

discharge of the glow or arc type, the discharge is maintained by the secondary electrons produced

at the cathode through various mechanisms, In the propagating current-sheet in this type of

accelerator, on the other hand, the ionization necessary for the maintenance of the discharge

is primarily due to the impact between the current-sheet and neutral atoms or molecules of

residual gas; therefore, the secondary electron emission from the cathode and the ionization

at the cathode fall are both unnecessary. Phis seems to introduce a lower cathode fall and a

non-conductive feature of the current flow to the cathode.
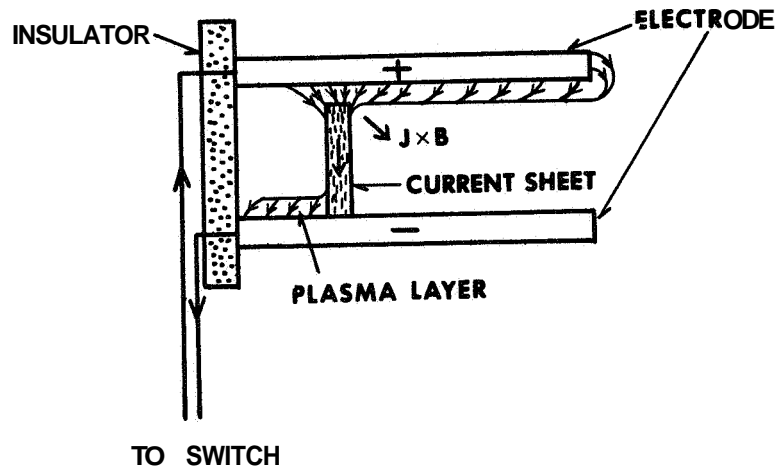
FIG. 12 SIMPLIFIED PATTERN OF CURRENT PATH IN THE CURRENT-SHEET

IV. Shape of current-sheet

The existence of an appreciable level of pre-ionization and of the surface current along the anode immediately results in a deviation of the current-sheet from the expected shape. It is well-known [7] [8] [9] that the current-sheet inclines toward the anode in a parallel plate accelerator. This can be explained as follows: since the current-sheet near the anode has a forward axial current component, this part of the sheet experiences a $\vec{j} \times \vec{B}$ force directed toward the cathode (see Fig. 12) and this tendency amplifies itself as the current-sheet travels down the electrode gap. This results in a current-sheet tilt as a whole., Lovberg observed [6] a planar current-sheet in the case of hydrogen filling (0.3 Torr) when the system is clean. As pointed out in the previous section, with hydrogen filling there is no appreciable pre-ionization and the axial current along the anode was not observed. This is considered to be the cause for the untilted current-sheet in this case.

In the coaxial accelerator, the level of pre-ionization and the forward axial current along the anode (outer electrode) vary sensitively with the ambient gas pressures, e.g., the axial current becomes small when $p > 1$ Torr for He, $p > 0.2$ Torr for N_2, and $p > 0.1$ Torr for A. The anode surface current should be restricted if the filling pressure of the working gases is high because of the low level of pre-ionization and this should introduce a pressure dependent behavior of the current-sheet; The shape (or inclination) of the electron density front which is sharply defined in the coaxial accelerator were determined by varying the gas pressure and the polarity of the electrodes with the optical arrangement shown in Fig. 4. The density front was found by observing the continuum intensity peak or by checking the spectral line intensity peak which gives the maximum width of the spectral line under observation. Typical oscillograms obtained with one monochromator at $r = r_1$ and the other at $r = r_2$, in the case of

hydrogen and argon filling, are shown in Fig. 13. This gives a delay time between the two signals when both are displayed simultaneously on the oscilloscope screen. Table 1 showing the polarity and the pressure dependence gives the propagation velocity of the leading front V and the distance d which is the separation between the density front at the center electrode and the outer electrode – d is derived from the delay time and the velocity. As can be seen, the density front is inclined or canted for all gases used regardless of its pressure if the center electrode is positive and roughly coincides with the luminous front observed in the framing photographs. When the center electrode is negative, however, a distinct pressure effect of gas can be seen, i.e., the density front is less canted or nearly flat when gas pressures are low, but with the higher gas pressure the front is inclined as much as in the positive case. This indicates that the flatter current-sheet is produced only when the gas pressures are low, where there is intense pre-ionization, and hence the current along the anode surface is most likely. Again, in the case of hydrogen filling (p > 0.3 Torr), it does not show a distinct polarity effect in agreement with previous works [2] [10] [11]
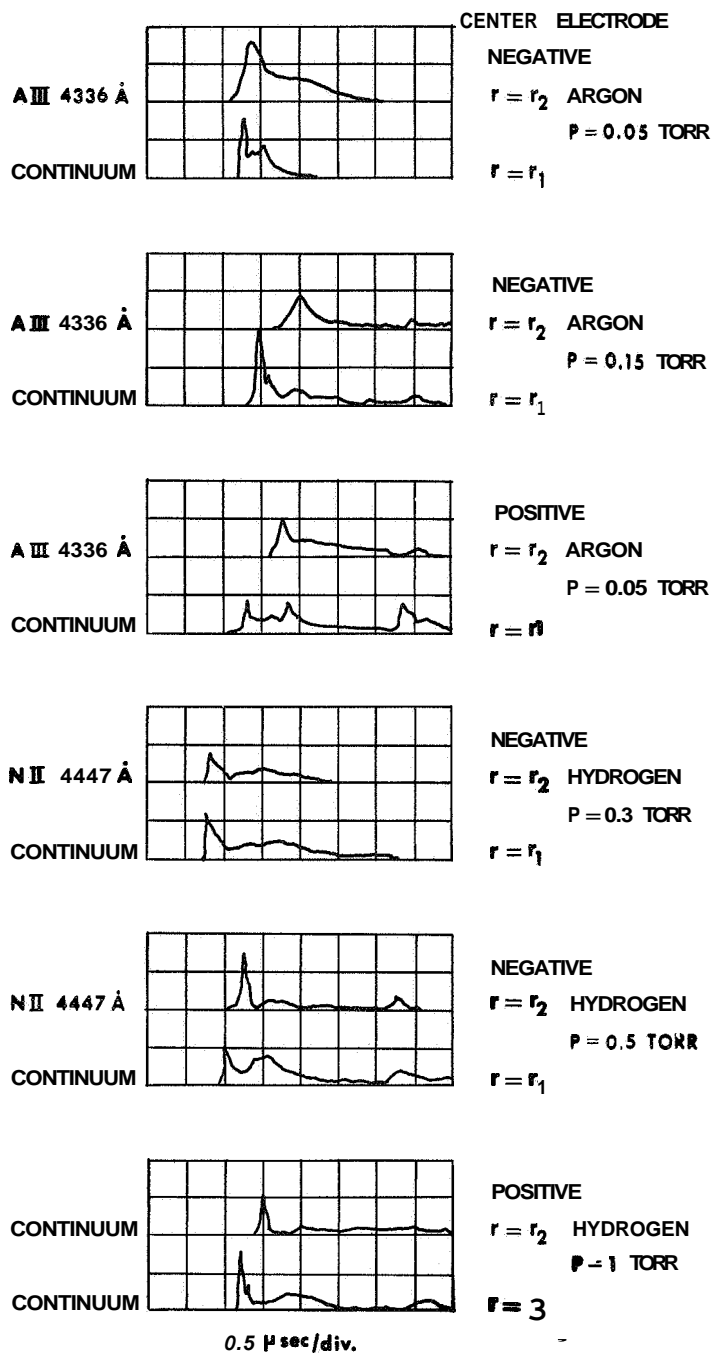
FIG. 13 SIMULTANEOUS RECORDINGS OF PHOTOELECTRIC SIGNALS FROM $r = r_1$ AND $r = r_2$ SHOWING TIME DELAY BETWEEN THEM (ARGON at $p = 0.05$, 0.15 TORR AND H_2 AT $p = 0.3$, 0.5, 1 TORR)

| GAS	P TORR	CENTER ELECTRODE POSITIVE		CENTER ELECTRODE NEGATIVE	
		V CM/μSEC	d CM	V CM/μSEC	d CM
H$_2$	0.3	19	4.2	20	~1-2
	0.5	13.5	4	12.5	2.5
	1.0	10	3.5	10	3
He	0.4	13.5	5.4	12.5	0-1.5*
	0.5	9.4	4.3	9	3.9
	1.0	8.6	4.5	8.1	3.6
N$_2$	0.07	11.5	5	11	0.8
	0.1	10	5	9.3	2
	0.2	9	4.5	8.6	4
A	0.05	12	4.4	12	1.8
	0.15	9.3	5.1	9.3	5.1

* UNSTABLE
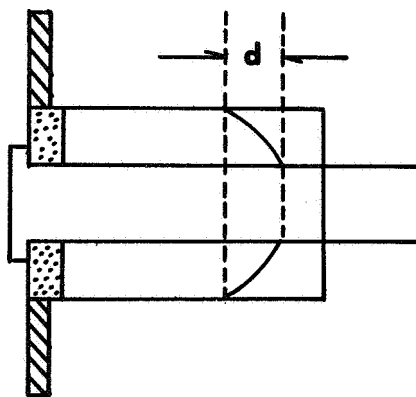
TABLE 1   POLARITY AND PRESSURE DEPENDENCE OF THE VELOCITY AND OF THE INCLINATION OF THE DENSITY FRONT

V. Calculation of Partition Function

In order to determine radiation loss, one has to know at least two quantities i.e.,
the particle density and the plasma temperature.   These quantities can be determined with
spectroscopic diagnostic techniques as shown in a previous report[12].   However, it is essential
that the relevant partition functions for any quantitative measurement be known.   The partition
function of an atom-like species,   a, at the ith stage of ionization is

$$Z^{a,i}(T) = \sum_{n=1}^{\infty} g_n e^{\frac{-E_n^{a,i}}{kT}} \quad ,$$

(1)

where g_n is the statistical weight, $2J+1$, of the level n whose energy, measured from
the ground state of the species is $E_n^{a,i}$. T is the absolute temperature and k is the
Boltzmann constant.   It is easy to see that the summation in Eq. 1 diverges.   However, for an
atom-like species surrounded by charged particles, as in a plasma, the summation in Eq. 1 is
usually terminated at a maximum principal quantum number, n_{max} where the excited electron
is still considered as a bound electron.   Thus for practical calculations of the partition function,
Eq. 1 now reads

$$Z^{a,i}(T) = \sum_{n=1}^{n=n_{max}} g_n e^{\frac{-E_n^{a,i}}{kT}} \quad .$$

(2)

The maximum principal quantum number, n_{max}, is related to the reduction of the ionization
energy[1], $\Delta E_\infty^{a,i}$, as

$$\Delta E_\infty^{a,i} = \frac{Z^2 E_\infty^H}{n_{max}^2}$$

(3)

where Z is the nuclear charge of the atom-like species ($Z=1$ for atoms, $Z=2$ for singly
ionized atoms   etc.). E_∞^H is the ionization energy of hydrogen.   Equation 3 results from the

fact that highly excited states near the ionization limit are sufficiently hydrogenic and can be described by hydrogenic formulae.

The reduction of the ionization energy, $\Delta E_\infty^{a,i}$, can be given[13] as

$$\Delta E_\infty^{a,i} = \frac{\rho e^2}{f_D} \quad \quad {}_3 \tag{4}$$

where f_D is the Debye radius and can be expressed as

$$f_D = \left[\frac{kT}{4\pi e^2 (N_e + \sum_{a,i} z^2 N_i^a)} \right]^{\frac{1}{2}}, \tag{5}$$

where N_e is the electron density and N_i^a is the ion density (N_1^a for singly, N_2^a for doubly ionized, etc.). Combining Eq. (4) and (5), one can express the reduction of the ionization energy, in units of eV, as

$$\Delta E_\infty^{a,i} = 1.74 \times 10^{-10} z \left(\frac{N_e'}{T_e} \right)^{\frac{1}{2}}, \tag{6}$$

where $N_e' = N_e + \sum_{a,i} z^2 N_i^a$ and T_e is the temperature in units of eV. It is apparent that for a given $\Delta E_\infty^{a,i}$ one can calculate n_{max} and finally the partition function. To do this the Atomic Energy Levels of Charlotte E. Moore[14] can be used. However, since the tabulated energy levels of reference 14 are not complete, the following procedures must be used in the evaluation of any partition function:

1. The energy levels which are missing in Ref. 14 must be accounted for. For example, for $n = 5$ one expects 5s, 5p, 5d, 5f and 5g. If 5d is missing, the wave number of 5p can be used for that of 5d and the statistical weight of 5d calculated,

2. If the tabulation in Ref. 14 is up to some n', where $n' \ll n_{max}$ the summation in Eq. 2 is broken into two parts, that

$$\sum_{n=1}^{n_{max}} = \sum_{n=1}^{n'} + \sum_{n=n'}^{n_{max}}$$

$\sum_{n=1}^{n=n'}$ is to be obtained by summing over all the discrete levels which are available in

Ref. 2 including the missing terms. As for $\sum_{n=n'}^{n=n_{max}}$ it can be replaced by an integral

whose value is

$$\sum_{n=n'}^{n_{max}} = \frac{2}{3}(2S_1+1)(2L_1+1)\, n_{max}^3\, e^{-\frac{E_\infty^{a,i} - \Delta E_\infty^{a,i}}{kT}} \, ,$$

where S_1, L_1 have the usual meaning and are the quantum numbers of the parent configuration.

$E_\infty^{a,i}$ is the ionization energy of the atom-like species whose partition function is calcu-

lated. Following these procedures, the partition function of He II and C II are shown in

Figs. 14 and 15 for a wide range of N'_e and T.
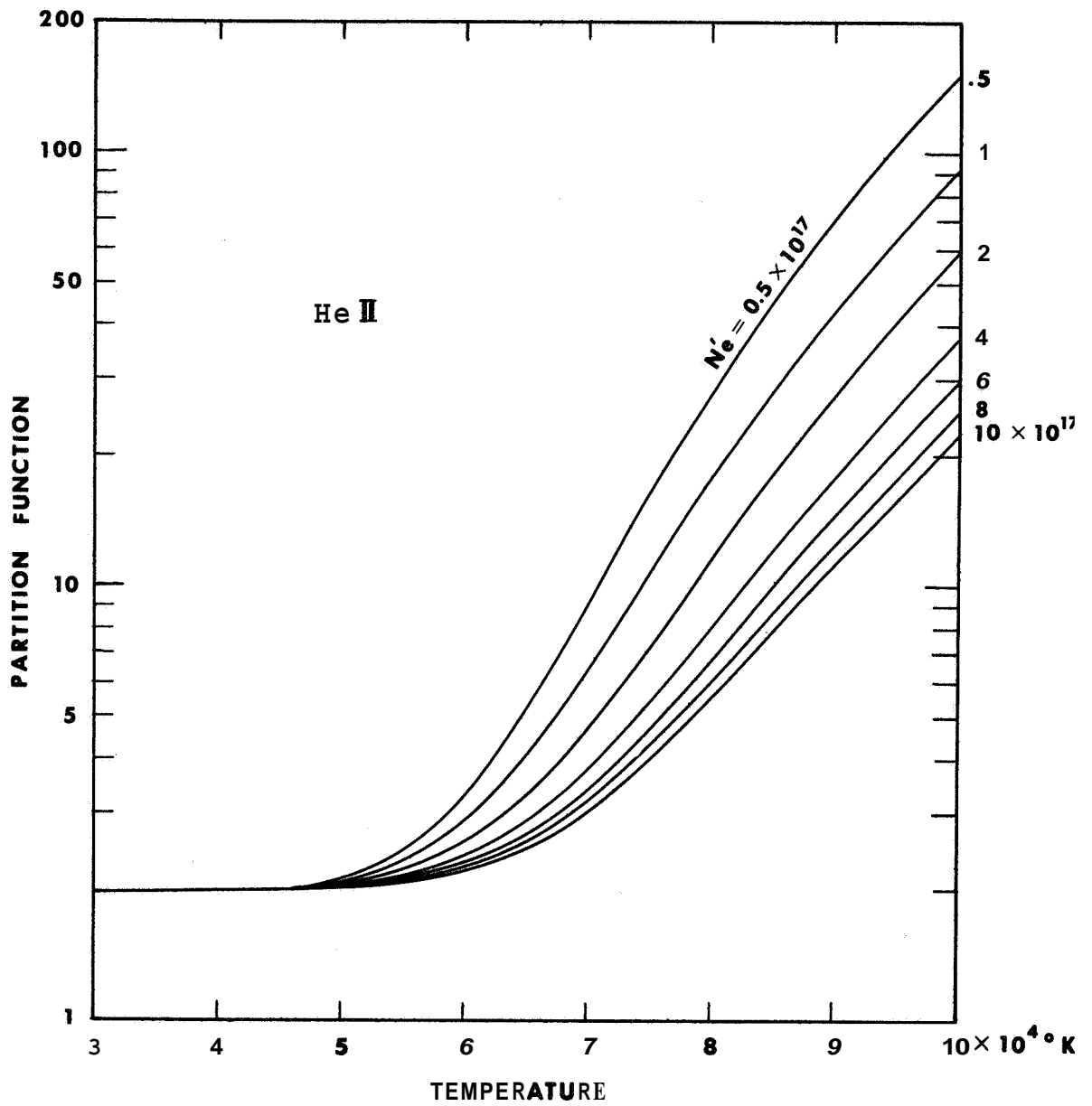
FIG.14   PARTITION   FUNCTION   OF   He II   AS   FUNCTION
OF   TEMPERATURE   FOR   VARIOUS N'_e
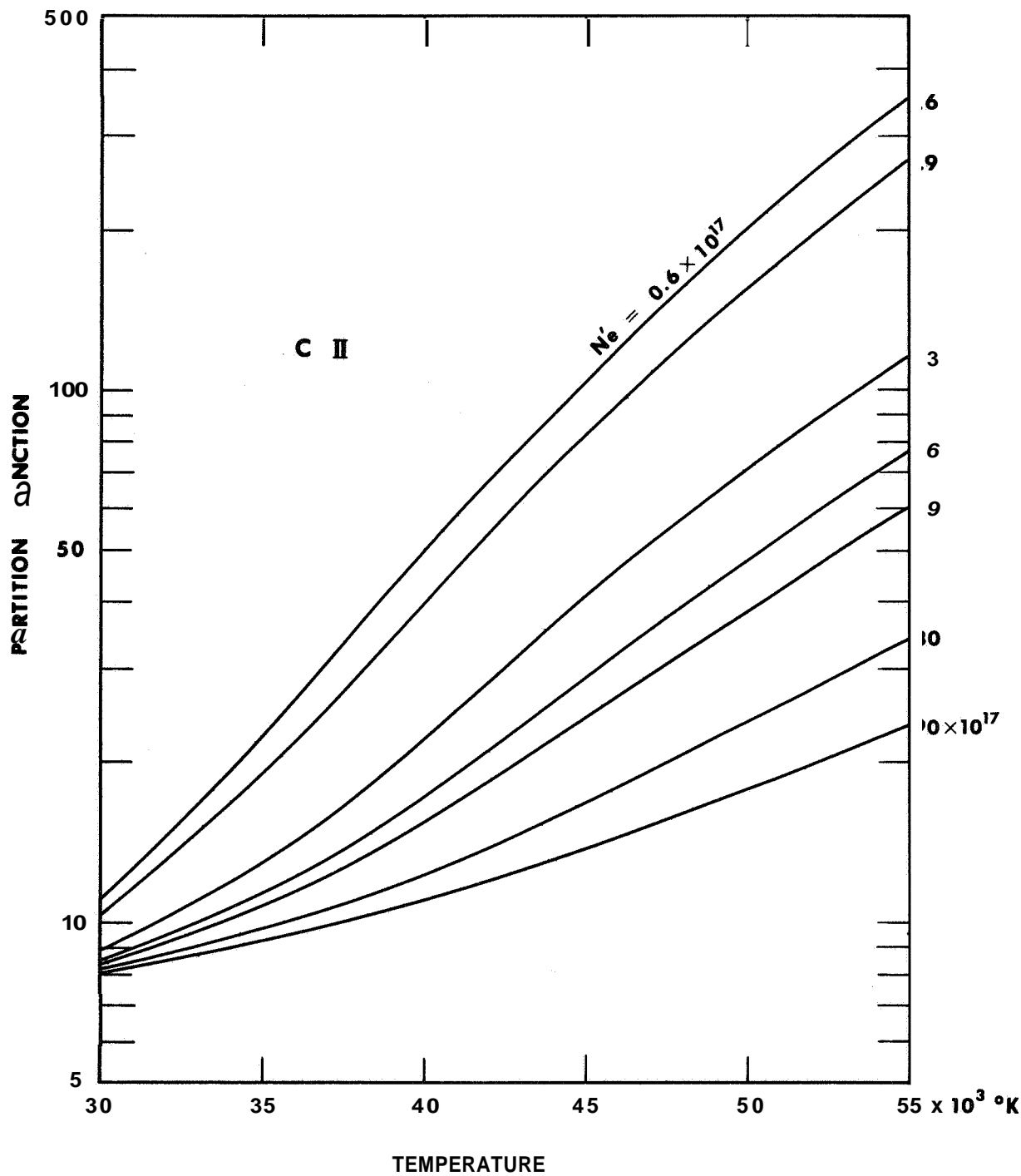
FIG.15   PARTITION FUNCTION OF C II FUNCTION OF
TEMPERATURE   FOR   VARIOUS N'_e

References

1. L. C. Burchhardt and R. H. Lovberg, Phys. Fluids $\underline{5}$ 341 (1962).

2. R. H. Lovberg, Phys. Fluids $\underline{8}$ 177 (1965).

3. J. C. Keck, Phys. Fluids $\underline{5}$ 630 (1962).

4. A. Dattner and J. Eninger, Phys. Fluids $\underline{7}$ S41 (1964).

5. M. J. Lubin, Phys. Fluids $\underline{10}$ 1794 (1967) .

6. R. H. Lovberg, Engrs. Trans Nucl. Sci. $\underline{NS-11}$ 187 (1964).

7. J. R. McLelland, A. S. V. Mackenzie, and J. Irving, Phys. Fluids $\underline{9}$ 1613 (1966).

8. R. H. Lovberg, AIAA Journal $\underline{4}$ 1215 (1966).

9. R. B. Johansson, Phys. Fluids $\underline{8}$ 866 (1965).

10. T. N. Lie, A. W. Ali, E.A. McLean and C. C. Chang, 2nd Semiannual Progress Report, NASA NGR-09-005-025, Department of Space Science and Applied Physics, Catholic University of America (1967).

11. J. W. Mather, Private Communication.

12. T. N. Lie, A. W. Ali, E. A. McLean, and A. C. Kolb, Phys. Fluids $\underline{10}$ 154.5 (1967).

13. H. R. Griem, "Plasma Spectroscopy" McGraw-Hill Book Co. New York 1964.

14. C. E. Moore, "Atomic Energy Levels" National Bureau of Standard (U.S.) circ. 467.

Project References

1. "Diagnostics of Accelerating Plasma"
   Research Proposal for NASA Research Grant NGR-09-005-025, Feb. 1965.

2. "Spectroscopic Study of a Coaxial Plasma Gun", Bulletin 10 523, American Physical Society Meeting in Washington, D. C. April 26-29, 1965.

3. "Diagnostics of Accelerating Plasma" Part V, 102
   Fifth NASA Intercenter Conference on Plasma Physics in Washington, D. C.,
   May 24-26, 1966.

4. "First Semi-Annual Progress Report for the period March 1 - Aug. 31, 1966,
   Research Grant NGR-09-005-025. Report No. 66-010, Department of Space Science
   & Applied Physics, Catholic University of America, Washington, D. C.

5. "Electric Polarity Effect in Coaxial Plasma Accelerator", Paper 7C-1, Eighth Annual
   Meeting on Plasma Physics of American Physical Society, Boston Nov. 2-5, 1966.

6. "Plasma State in Coaxial Accelerator", Physics of Fluids 10 1545 1967.

7. Second Semi-Annual Progress Report for the period September 1, 1966 - Feb. 28, 1967,
   Research Grant NGR-09-005-025
   Report No. 66-021, Department of Space Science & Applied Physics,
   Catholic University of America, Washington, D. C.

8. "Magnetohydrodynamic Shock Wave Structure" by C. K. Liu, (Ph .D. Thesis 1967),
   Report No. 67-028, Department of Space Science and Applied Physics, Catholic University of
   America, Washington, D. C.

9. "Studies of Current-Sheet in a Coaxial Plasma Accelerator" paper No, 67-658, AIAA Electric
   Propulsion and Plasmadynamics Conference, Colorado Springs, Sept. 11-13, 1967.

10. "Pre-ionization Phenomena in Pulsed Plasma Accelerator" paper E5, Proc. APS Topical
    Conference on Pulsed High-Density Plasmas, Los Alamos, Sept. 19-22, 1967.